SUPPORTING INFORMATION

Table S1. Year-specific mean area swept (sq. km) used as the model offset to predict probabilities of occurrence, numerical abundance, and biomass for Arrowtooth Flounder and Walleye Pollock in the Bering Sea (1982 to 2018).

Year	Area Swept (sq. km)	
	Mean	Std. Dev.
1982	0.044658	0.004174
1983	0.044639	0.005030
1984	0.044638	0.004372
1985	0.039067	0.007900
1986	0.045182	0.003855
1987	0.046507	0.004626
1988	0.043851	0.005710
1989	0.043260	0.008310
1990	0.042786	0.007404
1991	0.041187	0.008439
1992	0.044082	0.008305
1993	0.050082	0.007845
1994	0.045940	0.004765
1995	0.047910	0.006489
1996	0.046532	0.005264
1997	0.046552	0.005308
1998	0.049602	0.005635
1999	0.048639	0.006340
2000	0.046998	0.005773
2001	0.046261	0.005762
2002	0.044311	0.007393
2003	0.048512	0.007151
2004	0.044787	0.008302
2005	0.046227	0.006645
2006	0.048844	0.004806
2007	0.047561	0.004919
2008	0.044946	0.006175
2009	0.049678	0.005014
2010	0.044365	0.007170
2011	0.046220	0.005618
2012	0.043198	0.008475
2013	0.048029	0.004694
2014	0.047064	0.004440
2015	0.047470	0.005043
2016	0.043258	0.007208
2017	0.046473	0.004960
2018	0.046209	0.005418

Table S2. Environmental covariates included in each model type (S, D1, D2, D3) used to quantify and predict presence-absence, numerical abundance, or biomass for Arrowtooth Flounder and Walleye Pollock in the Bering Sea (1982 to 2018).Variables in bold denote those that are time-varying. All others represent spatially-explicit but long-term mean conditions. P/A = presence-absence. BPI = bathymetric position index.

Static (S)	Dynamic (D1)	Dynamic (D2)	Dynamic (D3)
Lon X Lat	Lon X Lat	Lon X Lat	Lon X Lat
		Year	**Year**
			Lon X Lat X Year
Depth (m)	Depth (m)	Depth (m)	Depth (m)
Slope	Slope	Slope	Slope
BPI	BPI	BPI	BPI
Sediment Grain Size (Φ)	Sediment Grain Size (Φ)	Sediment Grain Size (Φ)	Sediment Grain Size (Φ)
Bottom Temperature (°C)	**Bottom Temperature (°C)**	**Bottom Temperature (°C)**	**Bottom Temperature (°C)**
	Cold Pool Extent (km^2)	**Cold Pool Extent (km^2)**	**Cold Pool Extent (km^2)**
Sponge P/A	Sponge P/A	Sponge P/A	Sponge P/A
Coral P/A	Coral P/A	Coral P/A	Coral P/A
Whips P/A	Whips P/A	Whips P/A	Whips P/A
Area Swept (offset)	**Area Swept (offset)**	**Area Swept (offset)**	**Area Swept (offset)**

Table S3. Covariate effects on the probability of occurrence, b) numerical abundance, and c) biomass of Walleye Pollock (*Gadus chalcogrammus*) and Arrowtooth Flounder (*Atheresthes stomias*) in the Bering Sea (1982 to 2018). Results are from best-fit complex dynamic models only (spatially-explicit and time-varying covariates, spatial term, temporal term, spatiotemporal term). BPI: bathymetric position index, CPE: cold pool extent, P/A: presence or absence.

a) Probability of Occurrence

	Arrowtooth Flounder				Walleye Pollock			
	edf	Ref. df	χ^2	p	edf	Ref. df	χ^2	p
Year	8.80	9	249.7	< 0.001	8.75	9	274.8	< 0.001
Long, Lat	23.91	24	173.1	< 0.001	21.26	24	254.9	< 0.001
Long, Lat, Year	58.97	64	388.4	< 0.001	62.38	64	389.8	< 0.001
Depth (m)	4.94	5	294.9	< 0.001	4.97	5	416.8	< 0.001
Slope (°)	1.09	3	2.1	0.121	2.89	3	26.4	< 0.001
BPI	NA	NA	NA	NA	NA	NA	NA	NA
Bottom Temp. (°C)	2.92	3	80.1	< 0.001	2.53	3	24.1	< 0.001
Long, Lat:CPE	25.33	27	244.2	< 0.001	29.85	30	372.6	< 0.001
	Est.	SE	Z	p	Est.	SE	Z	p
Intercept	- 5.50	1.47	- 3.7	< 0.001	4.59	0.08	56.7	< 0.001
Sponges (P/A)	NA	NA	NA	NA	NA	NA	NA	NA
Corals (P/A)	- 0.36	0.12	- 3.1	0.002	- 0.20	0.08	- 2.5	0.014
Whips (P/A)	NA	NA	NA	NA	NA	NA	NA	NA

Table S3 (cont'd)**.** Covariate effects on the probability of occurrence, b) numerical abundance, and c) biomass of Walleye Pollock (*Gadus chalcogrammus*) and Arrowtooth Flounder (*Atheresthes stomias*) in the Bering Sea (1982 to 2018). Results are from best-fit complex dynamic models only (spatially-explicit and time-varying covariates, spatial term, temporal term, spatiotemporal term). BPI: bathymetric position index, CPE: cold pool extent, P/A: presence or absence.

b) Numerical Abundance

	Arrowtooth Flounder				Walleye Pollock			
	edf	Ref. df	χ^2	p	edf	Ref. df	χ^2	p
Year	8.97	9	1565	< 0.001	9.00	9	419209	< 0.001
Long, Lat	23.98	24	4743	< 0.001	24.00	24	344751	< 0.001
Long, Lat, Year	63.23	64	10133	< 0.001	63.95	64	769623	< 0.001
Depth (m)	4.99	5	13488	< 0.001	5.00	5	58948	< 0.001
Slope (°)	2.99	3	111	< 0.001	2.99	3	2480	< 0.001
BPI	NA	NA	NA	NA	3.00	3	9791	< 0.001
Bottom Temp. (°C)	2.99	3	775	< 0.001	3.00	3	10682	< 0.001
Long, Lat:CPE	29.90	30	3755	< 0.001	29.99	30	204012	< 0.001
	Est.	SE	Z	p	Est.	SE	Z	p
Intercept	6.00	0.01	435.0	< 0.001	8.84	0.00	3849.2	< 0.001
Sponges (P/A)	0.02	0.01	1.74	0.082	- 0.16	0.00	- 107.9	< 0.001
Corals (P/A)	- 0.29	0.01	- 24.20	< 0.001	0.09	0.00	29.1	< 0.001
Whips (P/A)	- 0.10	0.01	- 11.27	< 0.001	0.19	0.00	108.8	< 0.001

Table S3 (cont'd)**.** Covariate effects on the probability of occurrence, b) numerical abundance, and c) biomass of Walleye Pollock (*Gadus chalcogrammus*) and Arrowtooth Flounder (*Atheresthes stomias*) in the Bering Sea (1982 to 2018). Results are from best-fit complex dynamic models only (spatially-explicit and time-varying covariates, spatial term, temporal term, spatiotemporal term). BPI: bathymetric position index, CPE: cold pool extent, P/A: presence or absence.

c) Biomass

	Arrowtooth Flounder				Walleye Pollock			
	edf	Ref. df	F	p	edf	Ref. df	F	p
Year	8.44	9	6.79	< 0.001	8.93	9	47.82	< 0.001
Long, Lat	23.77	24	9.24	< 0.001	21.57	22	11.29	< 0.001
Long, Lat, Year	61.35	64	6.20	< 0.001	59.38	59	11.37	< 0.001
Depth (m)	4.92	5	126.35	< 0.001	4.66	5	21.40	< 0.001
Slope (°)	1.81	3	2.36	0.010	2.06	2	2.11	0.024
BPI	NA	NA	NA	NA	1.98	2	1.83	0.033
Bottom Temp. (°C)	2.85	3	7.19	< 0.001	2.51	3	5.91	< 0.001
Long, Lat:CPE	27.08	29	3.22	< 0.001	29.22	29	10.89	< 0.001
	Est.	SE	t	p	Est.	SE	t	p
Intercept	6.67	0.06	116.30	< 0.001	8.84	0.06	148.9	< 0.001
Sponges (P/A)	NA	NA	NA	NA	- 0.13	0.05	- 2.4	0.016
Corals (P/A)	- 0.39	0.07	- 5.63	< 0.001	- 0.38	0.10	- 3.9	< 0.001
Whips (P/A)	- 0.11	0.05	- 2.17	0.030	0.36	0.07	5.0	< 0.001

Table S4. Mean (± SD) correlations between retrospective forecasts and observations of Arrowtooth Flounder (*Atheresthes stomias*) and Walleye Pollock (*Gadus chalcogrammus*) in the Bering Sea (1982 to 2018). Spearman's correlation coefficients () are shown for probability of occurrence, numerical abundance, and biomass as estimated from S: static models (time-invariant and long-term mean habitat covariates, spatial term), D1: simple dynamic models (time-invariant and time-varying covariates, spatial term), D2: intermediate dynamic models (time-invariant and time-varying covariates, spatial term, temporal term), and D3: complex dynamic models (time-invariant and time-varying covariates, spatial term, temporal term, spatiotemporal term).

	Arrowtooth Flounder				Walleye Pollock			
Metric	S	D1	D2	D3	S	D1	D2	D3
Prob. Occur	0.76 (0.07)	0.60 (0.19)	0.58 (0.16)	0.57 (0.18)	0.36 (0.15)	0.17 (0.17)	0.17 (0.17)	0.12 (0.17)
Abundance	0.77 (0.07)	0.35 (0.35)	0.26 (0.43)	0.15 (0.42)	0.50 (0.20)	0.51 (0.17)	0.36 (0.27)	0.25 (0.23)
Biomass	0.78 (0.06)	0.65 (0.19)	0.68 (0.13)	0.65 (0.15)	0.48 (0.19)	0.42 (0.16)	0.39 (0.19)	0.29 (0.18)

Table S5. Minimum, mean (± SD), and maximum bottom temperatures (°C) used to quantify distributions and densities for Arrowtooth Flounder and Walleye Pollock in the Bering Sea (1982 to 2018). Values were obtained from regional ocean modeling system (ROMS) hindcasts (Hermann *et al.* 2013; Kearney *et al.* 2020) and are listed for the full time series used to fit models (P/A: presence-absence, Pos: positive catches in terms of numerical abundance or biomass) and those used to forecast population metrics.

	Min	Mean (SD)	Max
P/A (both species)	- 2.07	2.25 (2.01)	12.80
Pos. Arrowtooth Flounder	- 1.14	3.08 (1.23)	6.11
Pos. Walleye Pollock	- 2.07	2.12 (1.78)	12.80
Static Forecasts	- 1.75	2.56 (2.50)	12.08
Dynamic Forecasts	- 2.42	2.56 (2.77)	15.28

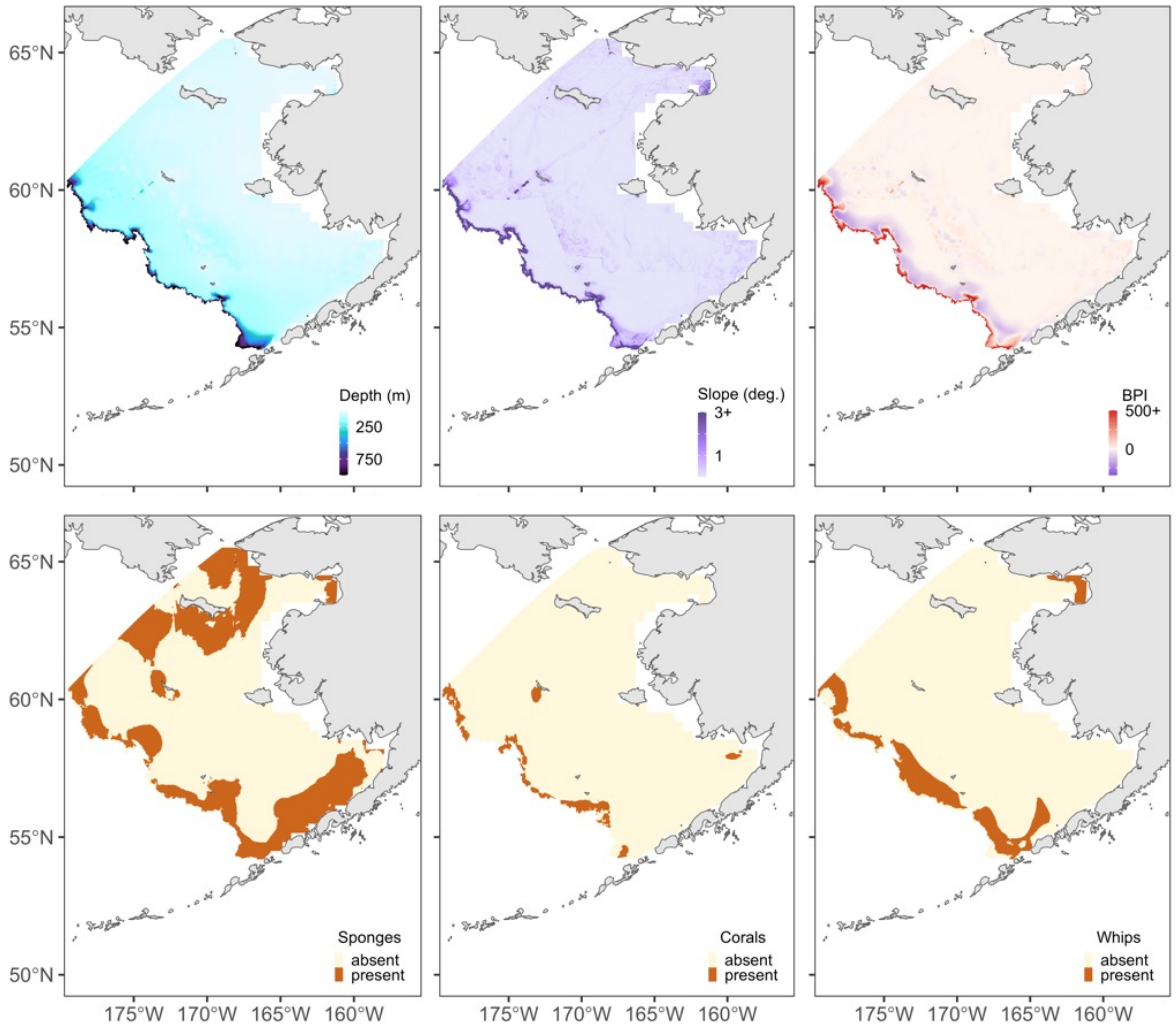

Figure S1. Static model covariates used to quantify probabilities of occurrence, numerical abundance, and biomass of Arrowtooth Flounder and Walleye Pollock in the Bering Sea (1982 to 2018). Clockwise from top left: depth (m), slope (degrees), bathymetric position index (BPI, unitless), sea whips and sea pens (Octocorallia spp., presence-absence), corals (Anthozoa spp., presence-absence), sponges (Porifera spp., presence-absence). Due to high concurvity with location, sediment grain size (phi; not shown) was excluded from all models.

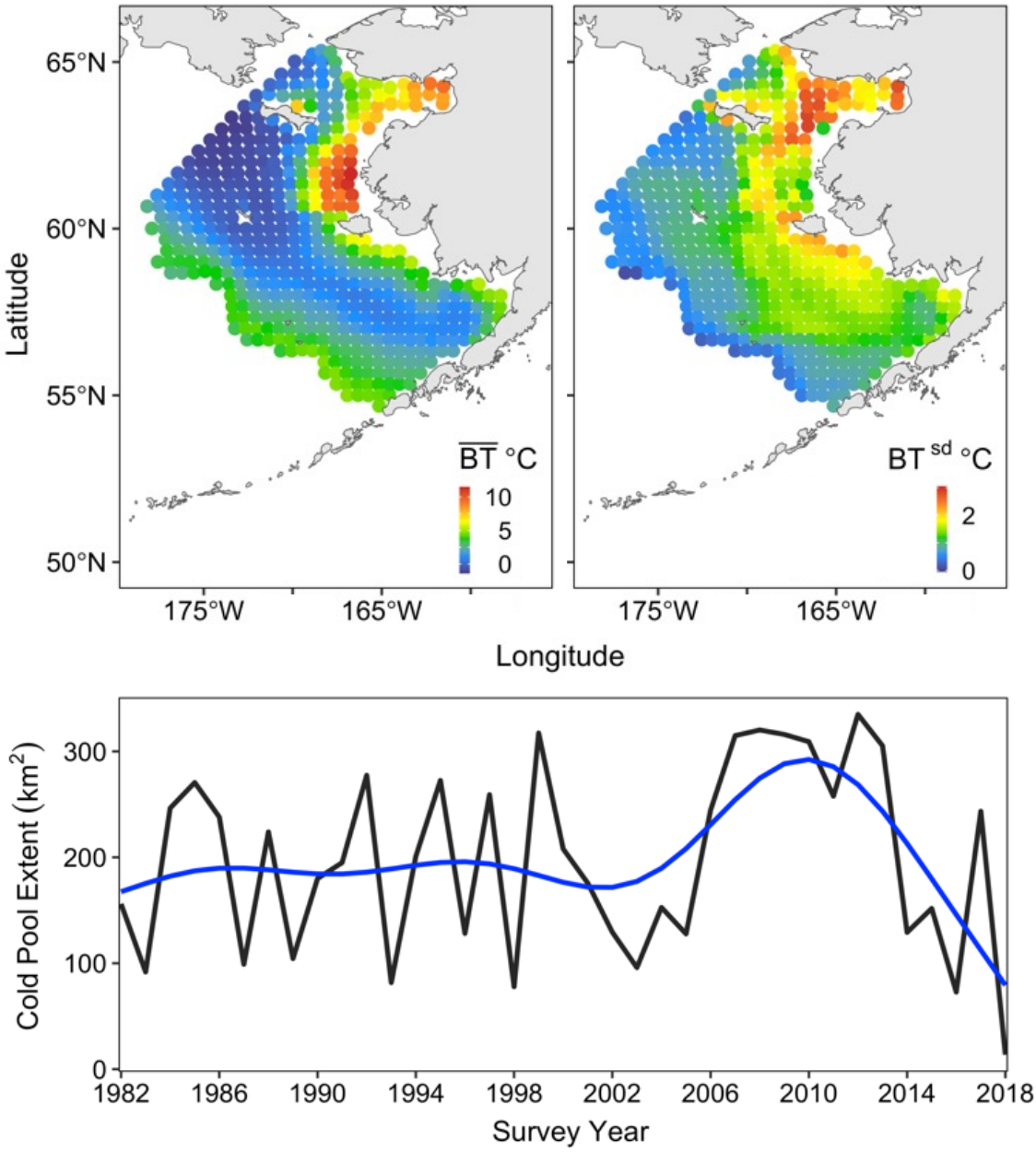

Figure S2. Dynamic model covariates used to quantify probabilities of occurrence, numerical abundance, and biomass of Arrowtooth Flounder and Walleye Pollock in the Bering Sea (1982 to 2018). Top left: Long-term mean bottom temperature (BT, °C). Top right: Standard deviations for bottom temperature across years (BT, °C). Bottom: Year-specific cold pool extent (sq. km; black: "observed", blue: "predicted"). All data were obtained from regional ocean modeling system (ROMS) hindcasts (Hermann *et al.* 2013; Kearney *et al.* 2020).

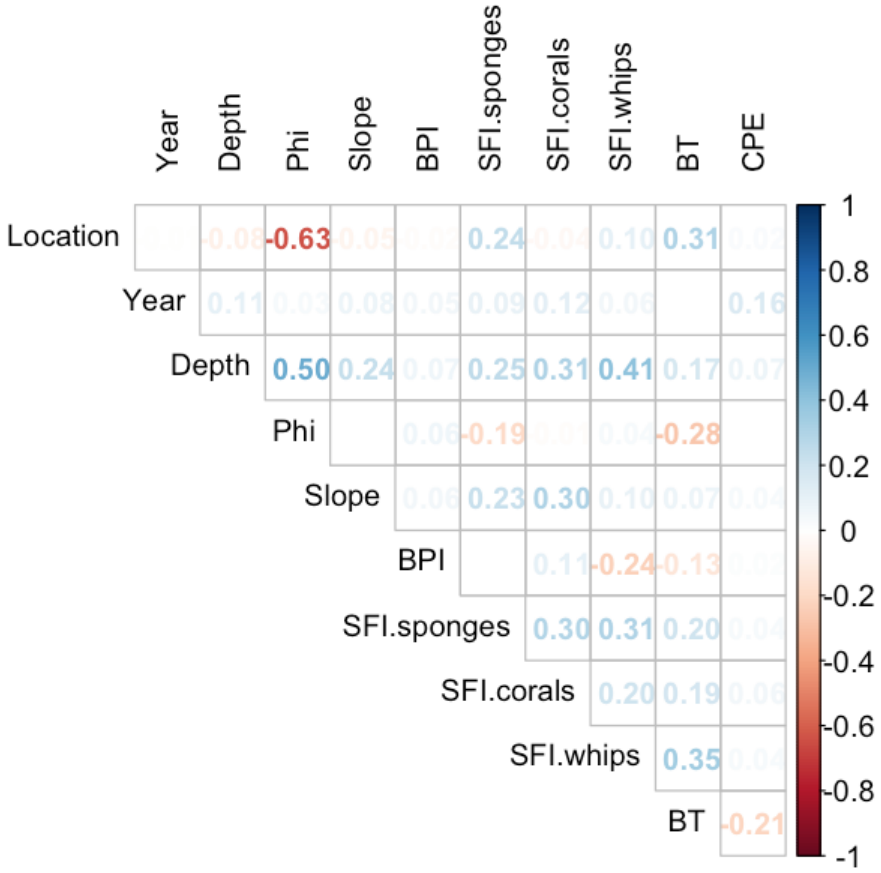

Figure S3. Spearman's correlations among environmental covariates used to model groundfish population metrics in the Bering Sea. Numbers indicate significant linear correlations ($y\alpha$ = 0.1), with warm colors denoting negative correlations and cool colors denoting positive correlations. Location (Lon X Lat), Depth (m), Phi: sediment grain size (Φ), BPI: bathymetric position index; BT: bottom temperature (°C); CPE: cold pool extent (km^2); SFI: occurrence of structure-forming invertebrates. Estimates of concurvity (a generalization of collinearity) was used to eliminate environmental covariates from Generalized Additive Models. Thus, Spearman's correlations are for illustrative purposes only.

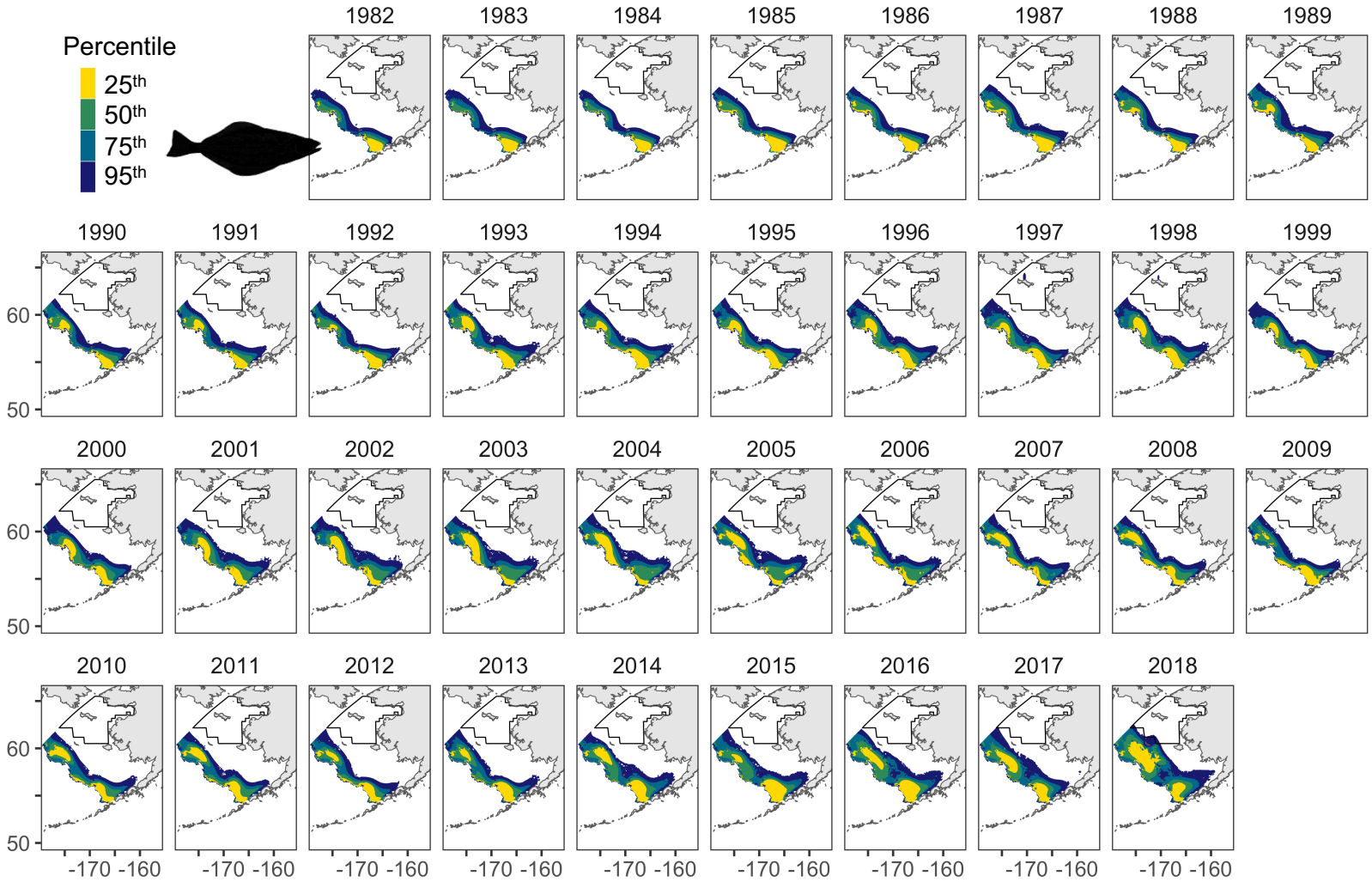

Figure S4. Population percentiles based on probability of occurrence from complex dynamic models for Arrowtooth Flounder in the Bering Sea (1982 to 2018). Yellow illustrates the top 25th percentile (categorized as "hot spots"); green shows the top 50th percentile ("core" habitat); teal represents the top 75th percentile ("principal" habitat); blue identifies the top 95th percentile (essential fish habitat [EFH]). The black outlined polygon denotes the northern Bering Sea, which was not sampled regularly throughout the time series.

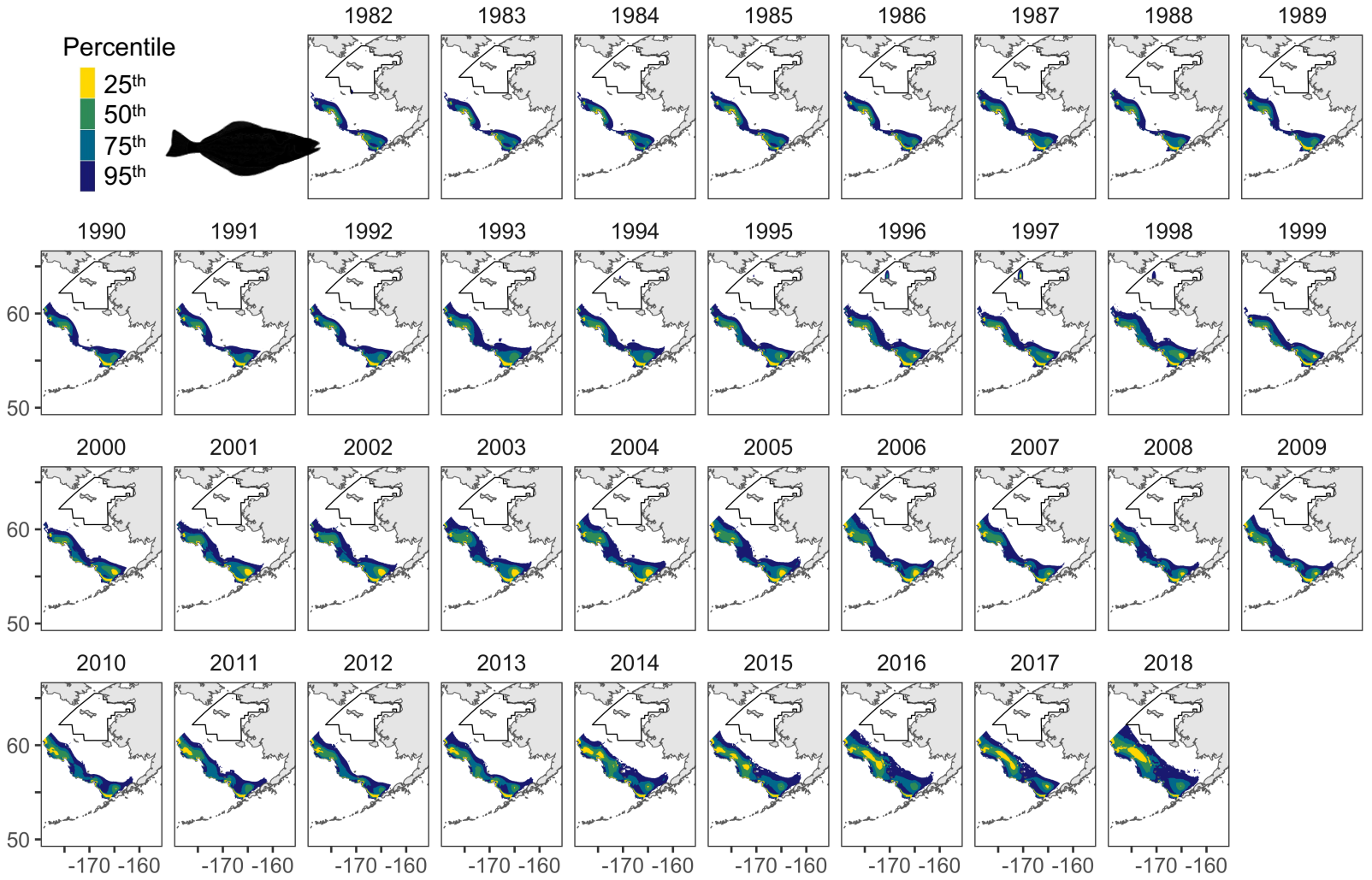

Figure S5. Population percentiles based on numerical abundance from complex dynamic models for Arrowtooth Flounder in the Bering Sea (1982 to 2018). Yellow illustrates the top 25th percentile (categorized as “hot spots”); green shows the top 50th percentile (“core” habitat); teal represents the top 75th percentile (“principal” habitat); blue identifies the top 95th percentile (essential fish habitat [EFH]). The black outlined polygon denotes the northern Bering Sea, which was not sampled regularly throughout the time series.

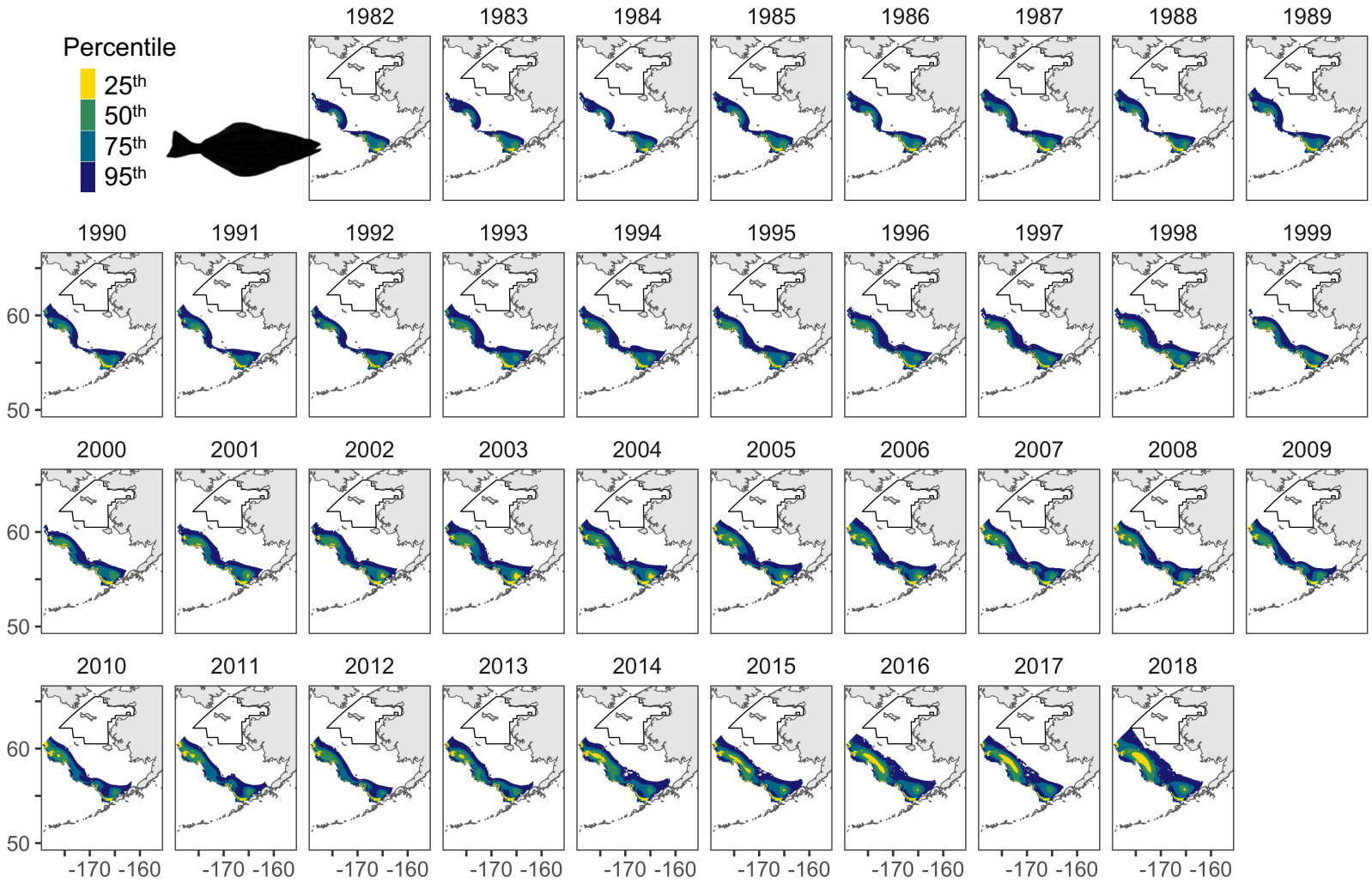

Figure S6. Population percentiles based on biomass from complex dynamic models for Arrowtooth Flounder in the Bering Sea (1982 to 2018). Yellow illustrates the top 25th percentile (categorized as “hot spots”); green shows the top 50th percentile (“core” habitat); teal represents the top 75th percentile (“principal” habitat); blue identifies the top 95th percentile (essential fish habitat [EFH]). The black outlined polygon denotes the northern Bering Sea, which was not sampled regularly throughout the time series.

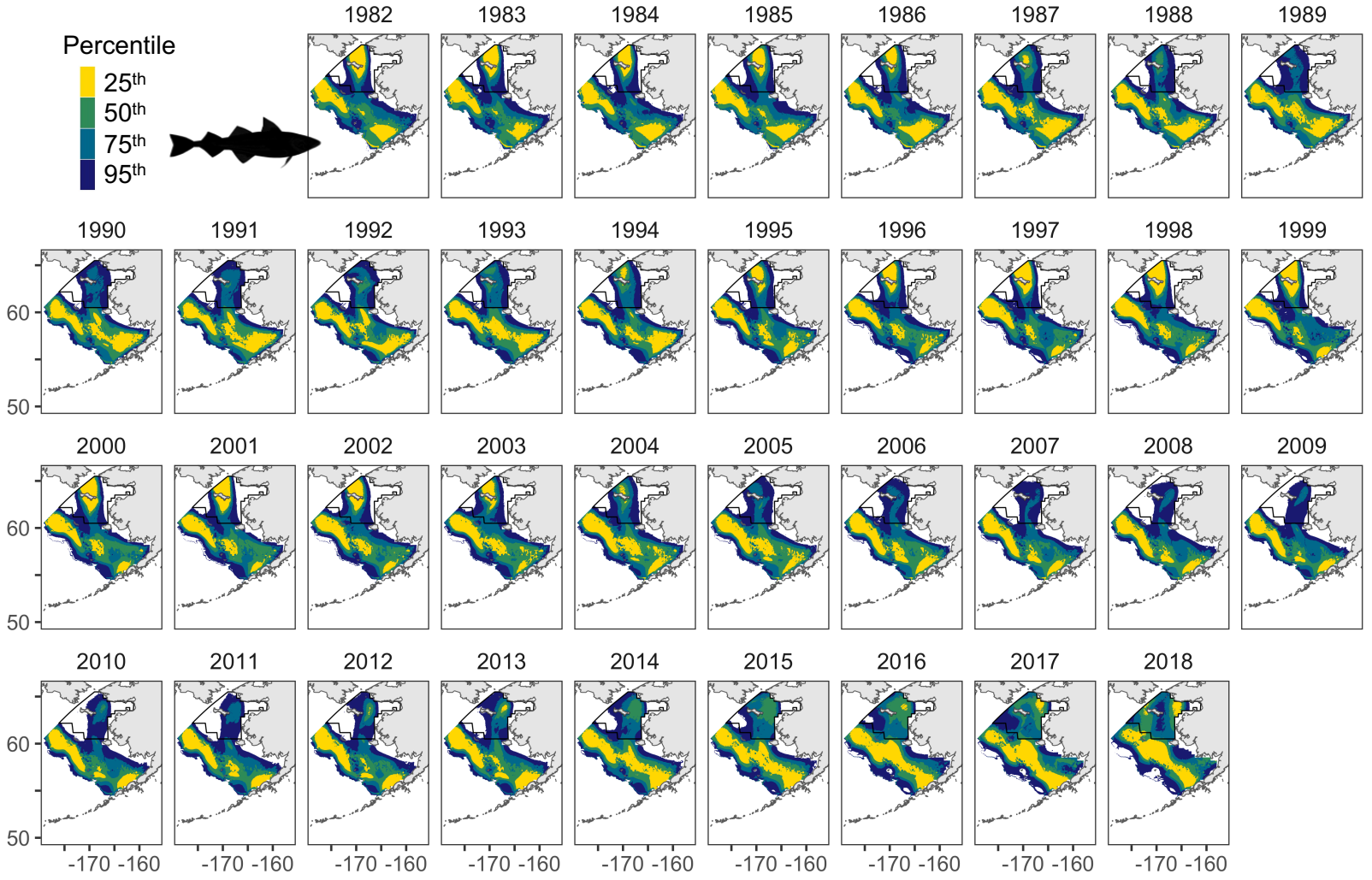

Figure S7. Population percentiles based on probability of occurrence from complex dynamic models for Walleye Pollock in the Bering Sea (1982 to 2018). Yellow illustrates the top 25th percentile (categorized as “hot spots”); green shows the top 50th percentile (“core” habitat); teal represents the top 75th percentile (“principal” habitat); blue identifies the top 95th percentile (essential fish habitat [EFH]). The black outlined polygon denotes the northern Bering Sea, which was not sampled regularly throughout the time series.

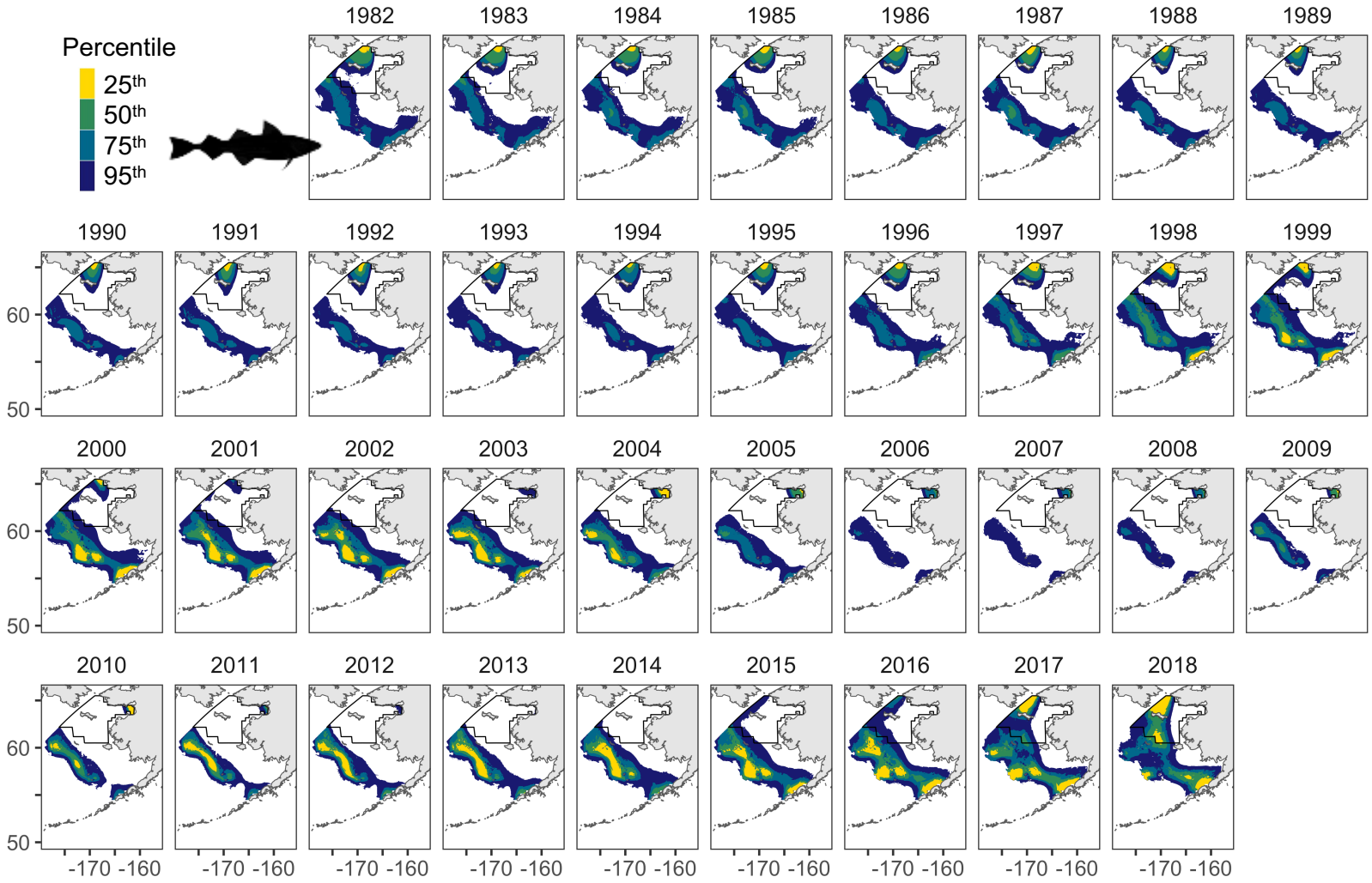

Figure S8. Population percentiles based on numerical abundance from complex dynamic models for Walleye Pollock in the Bering Sea (1982 to 2018). Yellow illustrates the top 25th percentile (categorized as "hot spots"); green shows the top 50th percentile ("core" habitat); teal represents the top 75th percentile ("principal" habitat); blue identifies the top 95th percentile (essential fish habitat [EFH]). The black outlined polygon denotes the northern Bering Sea, which was not sampled regularly throughout the time series.

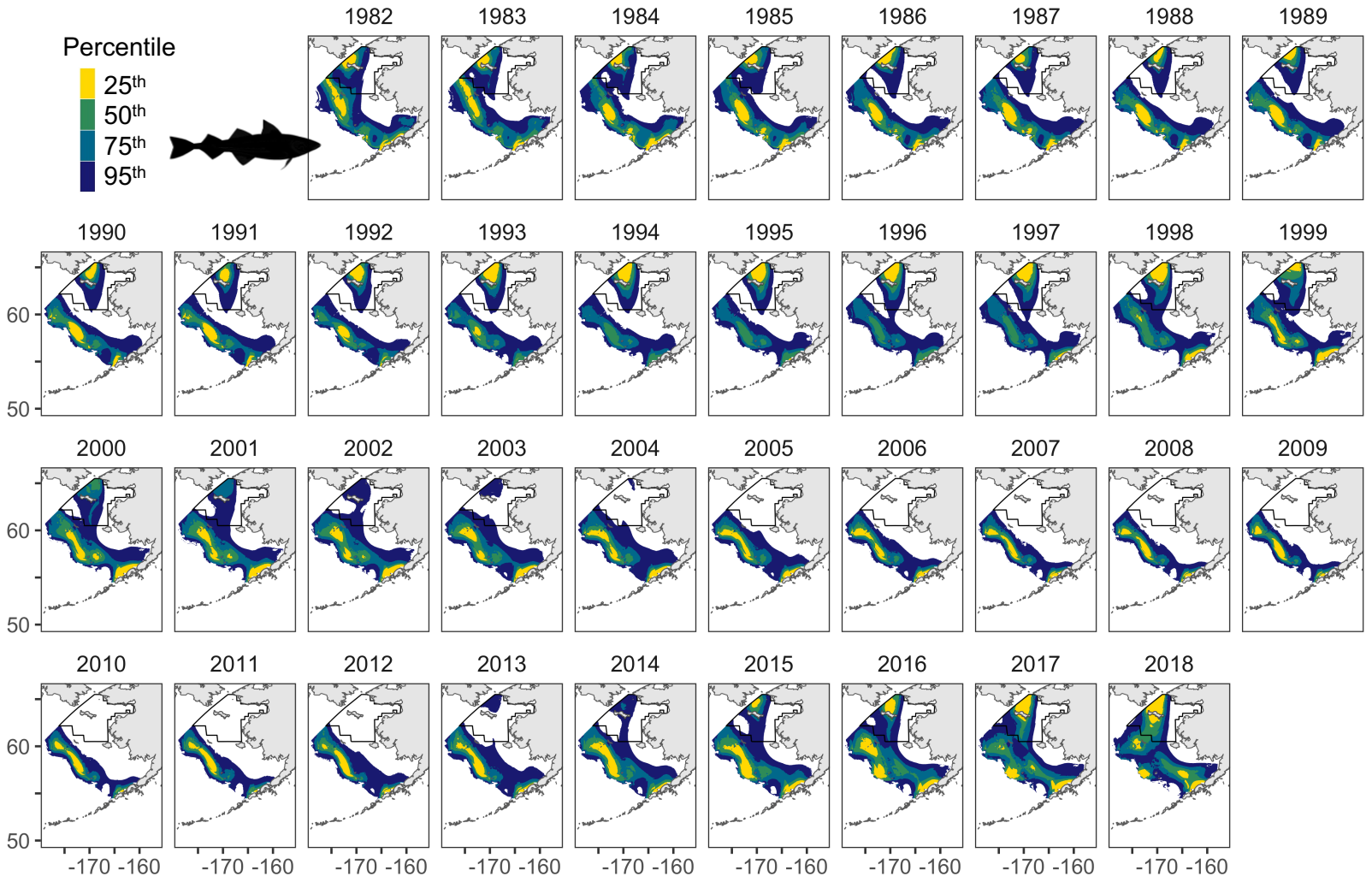

Figure S9. Population percentiles based on biomass from complex dynamic models for Walleye Pollock in the Bering Sea (1982 to 2018). Yellow illustrates the top 25th percentile (categorized as "hot spots"); green shows the top 50th percentile ("core" habitat); teal represents the top 75th percentile ("principal" habitat); blue identifies the top 95th percentile (essential fish habitat [EFH]). The black outlined polygon denotes the northern Bering Sea, which was not sampled regularly throughout the time series.

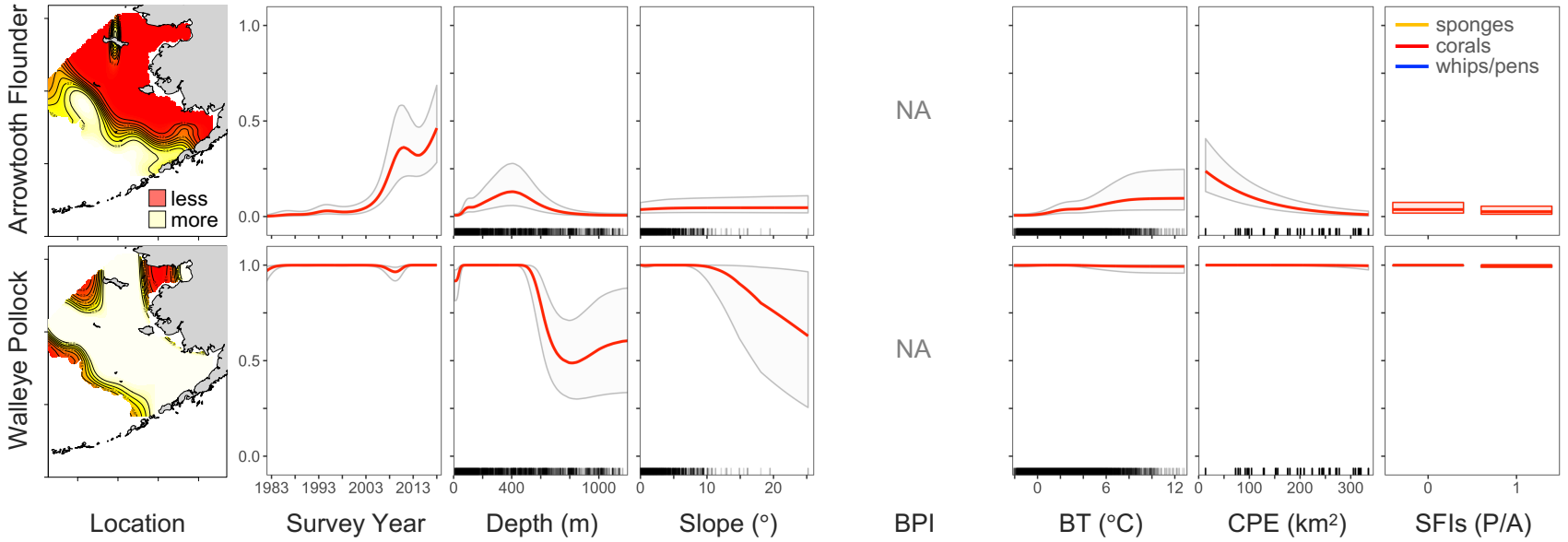

Figure S10. Partial covariate effects on the probability of occurrence for Arrowtooth Flounder (*Atheresthes stomias;* 381 mm) and Walleye Pollock (*Gadus chalcogrammus;* 250 mm). Results are from complex dynamic models only, which also included smoothed terms for spatiotemporal variation and spatially varying cold pool extent (included here as a one-dimensional effect for illustration purposes only). BPI: bathymetric position index; BT: bottom temperature; CPE: cold pool extent; SFI: structure-forming invertebrates (0 = absent, 1 = present); NA: not applicable (excluded from the final model).

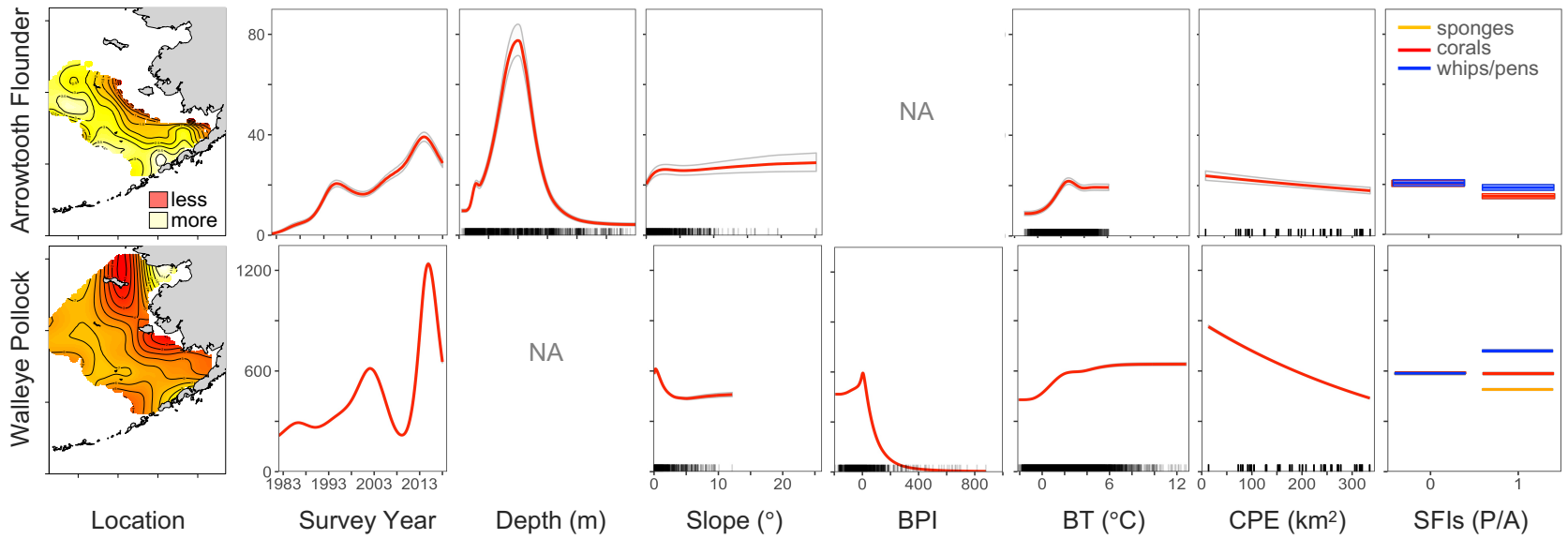

Figure S11. Partial covariate effects on the numerical abundance of Arrowtooth Flounder (*Atheresthes stomias;* 381 mm) and Walleye Pollock (*Gadus chalcogrammus;* 250 mm). Results are from complex dynamic models only, which also included smoothed terms for spatiotemporal variation and spatially varying cold pool extent (included here as a one-dimensional effect for illustration purposes only). BPI: bathymetric position index; BT: bottom temperature; CPE: cold pool extent; SFI: structure-forming invertebrates (0 = absent, 1 = present); NA: not applicable (excluded from the final model).

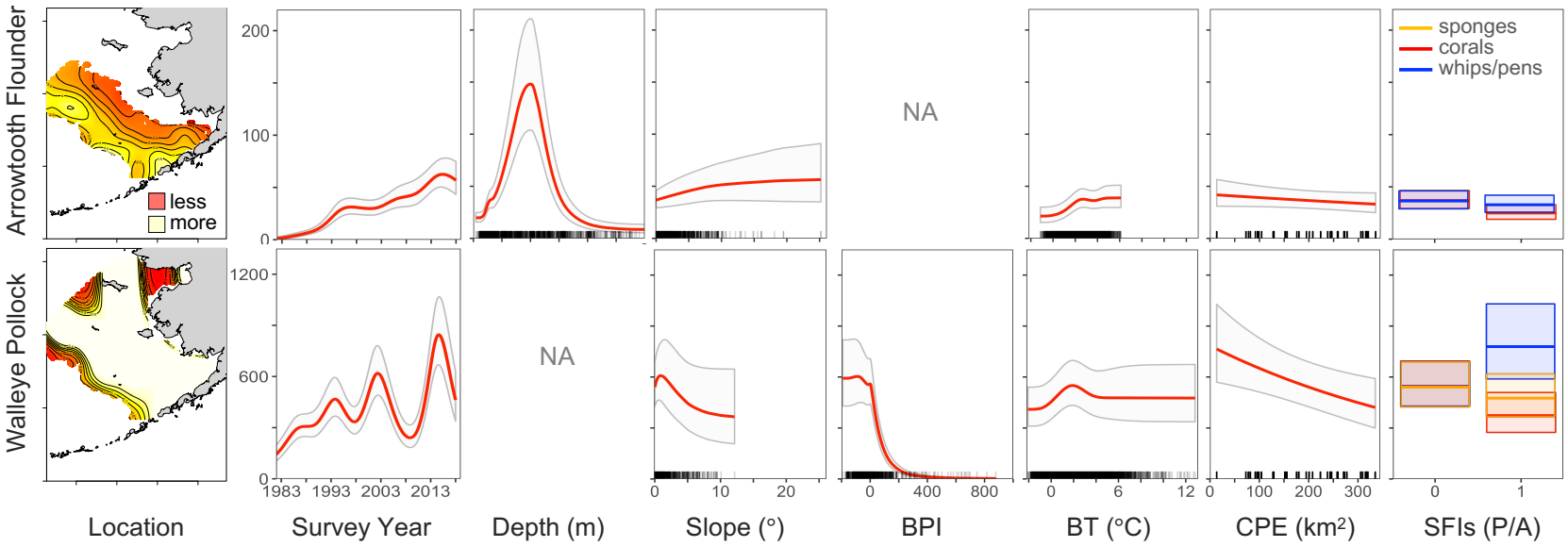

Figure S12. Partial covariate effects on the biomass of Arrowtooth Flounder (*Atheresthes stomias;* 381 mm) and Walleye Pollock (*Gadus chalcogrammus;* 250 mm). Results are from complex dynamic models only, which also included smoothed terms for spatiotemporal variation and spatially varying cold pool extent (included here as a one-dimensional effect for illustration purposes only). BPI: bathymetric position index; BT: bottom temperature; CPE: cold pool extent; SFI: structure-forming invertebrates (0 = absent, 1 = present); NA: not applicable (excluded from the final model).

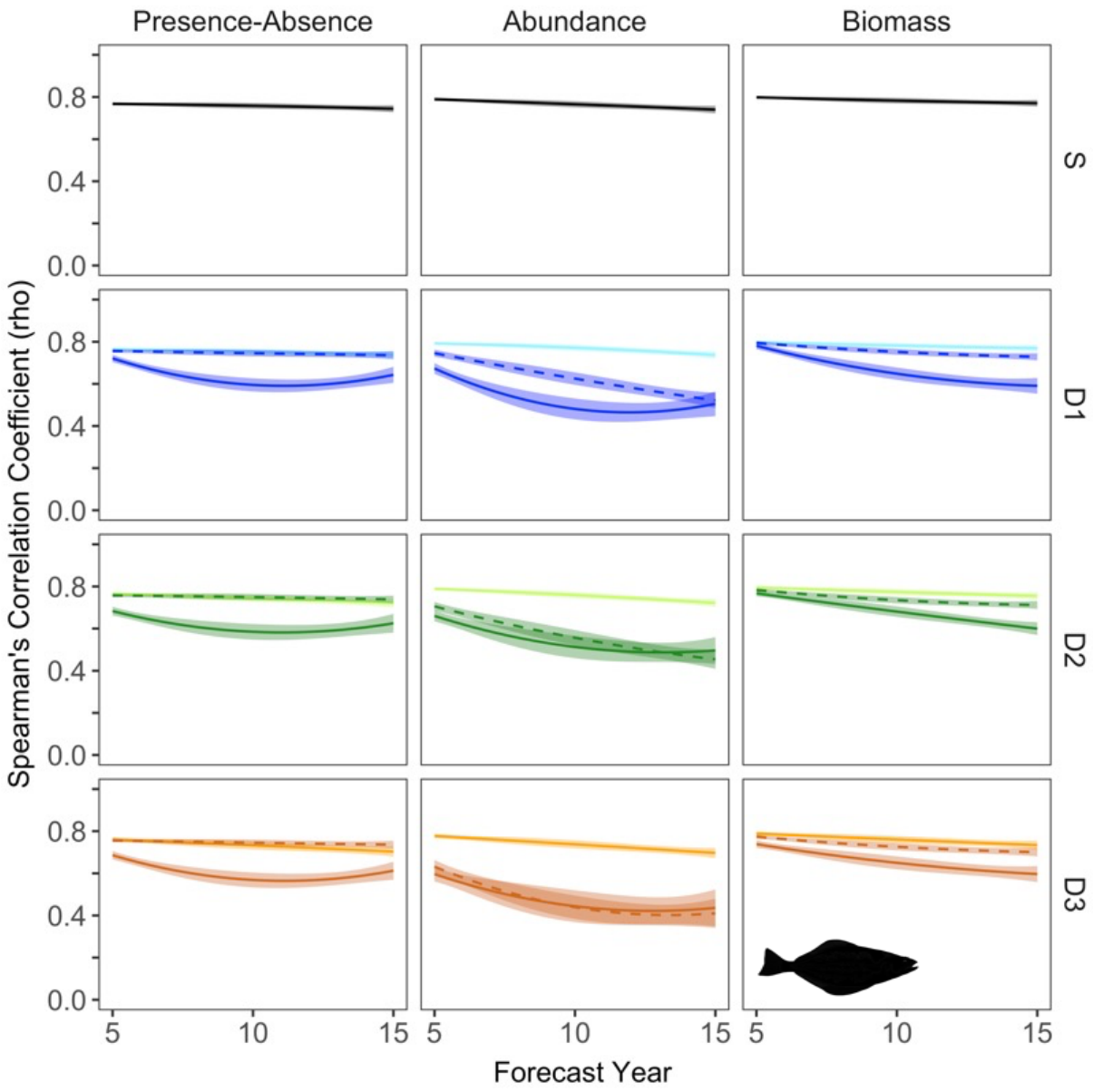

Figure S13. Spearman's correlation coefficients (ρ) for Arrowtooth Flounder presence-absence (left), abundance (center), and biomass (right). Means (solid lines) and standard deviations (bands) are shown for each model configuration (S: static, D1: simple dynamic, D2: intermediate dynamic, and D3: complex dynamic). Forecast years represent 10-yr moving windows (*e.g.*, forecast year 10 denotes mean correlations between observations and forecasts 6 to 15 years into the "future"). Solid lines with darker colors illustrate correlations between observations and forecasts from best-fit models. Dashed lines represent correlations using persistence forecasts from best-fit models (*i.e.*, all forecasts are identical to predictions based on the final year used for model fitting). Lighter colors demonstrate correlations between observations and forecasts when replacing time-varying temperatures with long-term means.

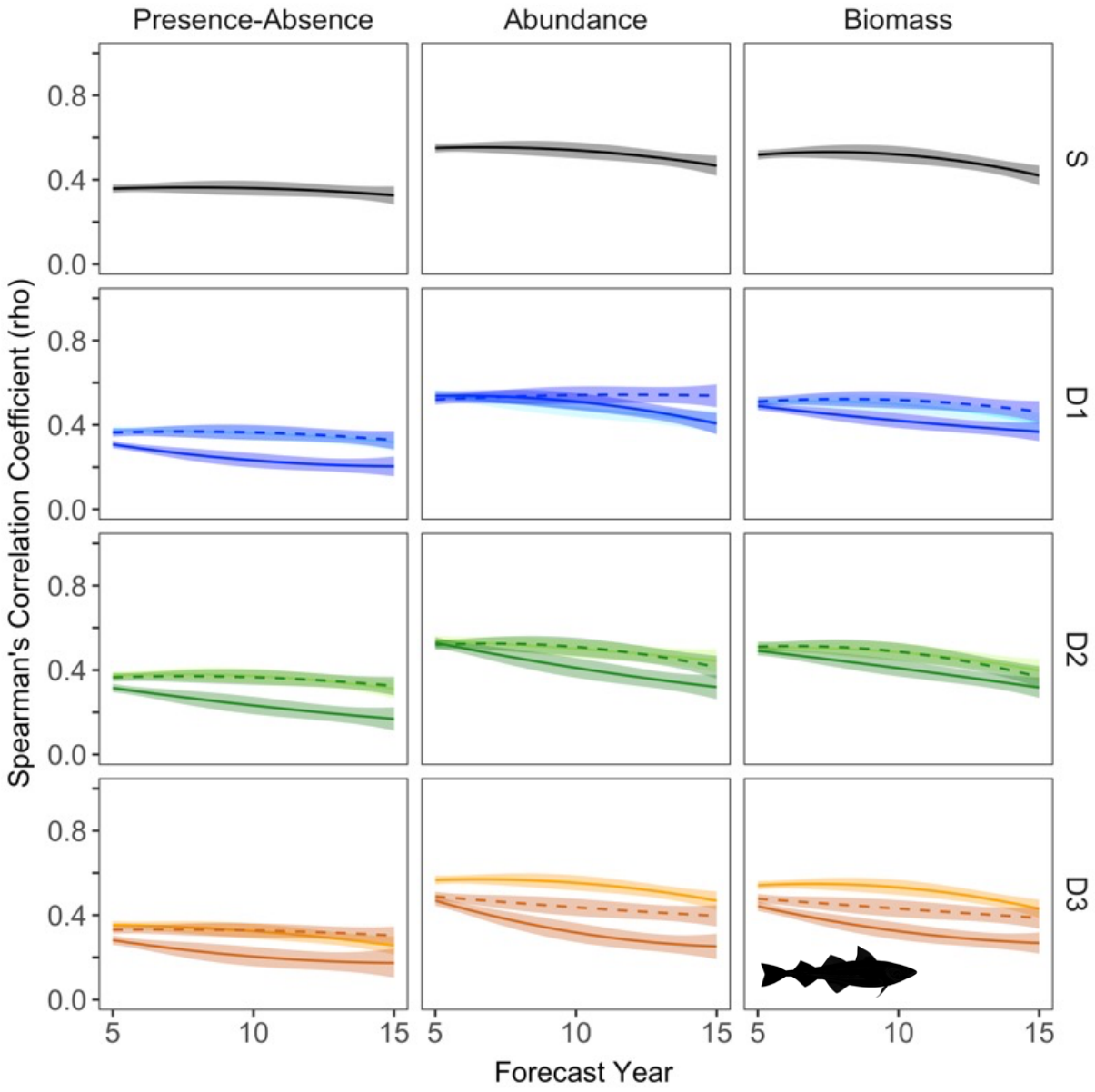

Figure S14. Spearman's correlation coefficients (ρ) for Walleye Pollock presence-absence (left), abundance (center), and biomass (right). Means (solid lines) and standard deviations (bands) are shown for each model configuration (S: static, D1: simple dynamic, D2: intermediate dynamic, and D3: complex dynamic). Forecast years represent 10-yr moving windows (*e.g.*, forecast year 10 denotes mean correlations between observations and forecasts 6 to 15 years into the "future"). Solid lines with darker colors illustrate correlations between observations and forecasts from best-fit models. Dashed lines represent correlations using persistence forecasts from best-fit models (*i.e.*, all forecasts are identical to predictions based on the final year used for model fitting). Lighter colors demonstrate correlations between observations and forecasts when replacing time-varying temperatures with long-term means.

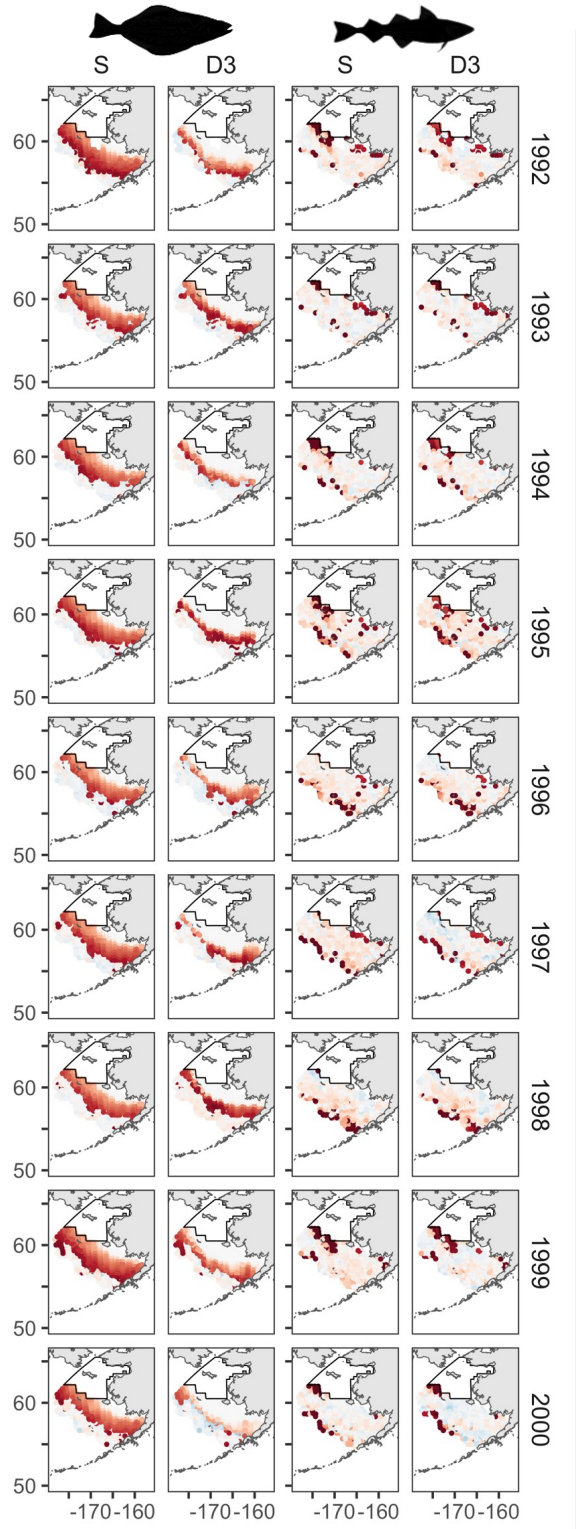

Figure S15. Standardized residuals from static (S) and complex dynamic (D3) models used to quantify biomass (kg) for Arrowtooth Flounder (left) and Walleye Pollock (right) in the Bering Sea. Years represent 1-yr forecasts beyond the time series fit (*e.g.,* 1992 was forecasted from models fit to data between 1982 and 1991). Blue: models underpredicted relative to observations. Red: models overpredicted relative to observations. The black outlined polygon denotes the northern Bering Sea, which was not regularly sampled in time and space.

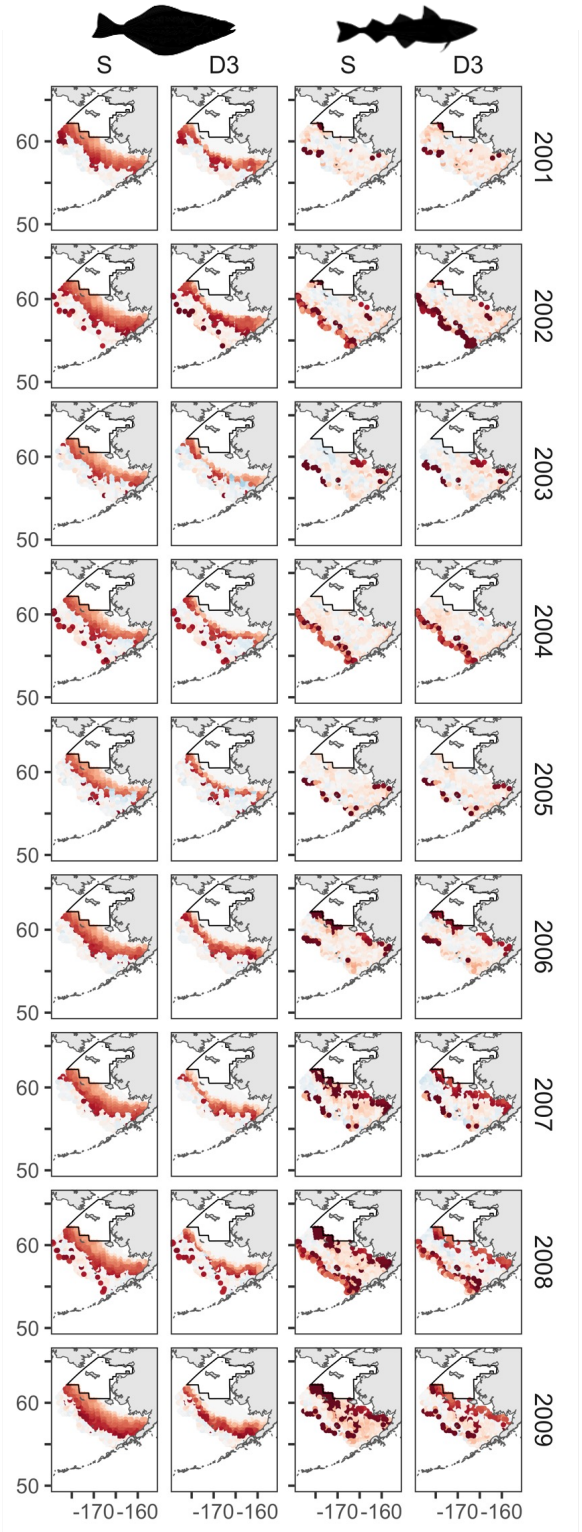

Figure S15 (cont'd). Standardized residuals from static (S) and complex dynamic (D3) models used to quantify biomass (kg) for Arrowtooth Flounder (left) and Walleye Pollock (right) in the Bering Sea. Years represent 1-yr forecasts beyond the time series fit (*e.g.,* 1992 was forecasted from models fit to data between 1982 and 1991). Blue: models underpredicted relative to observations. Red: models overpredicted relative to observations. The black outlined polygon denotes the northern Bering Sea, which was not regularly sampled in time and space.

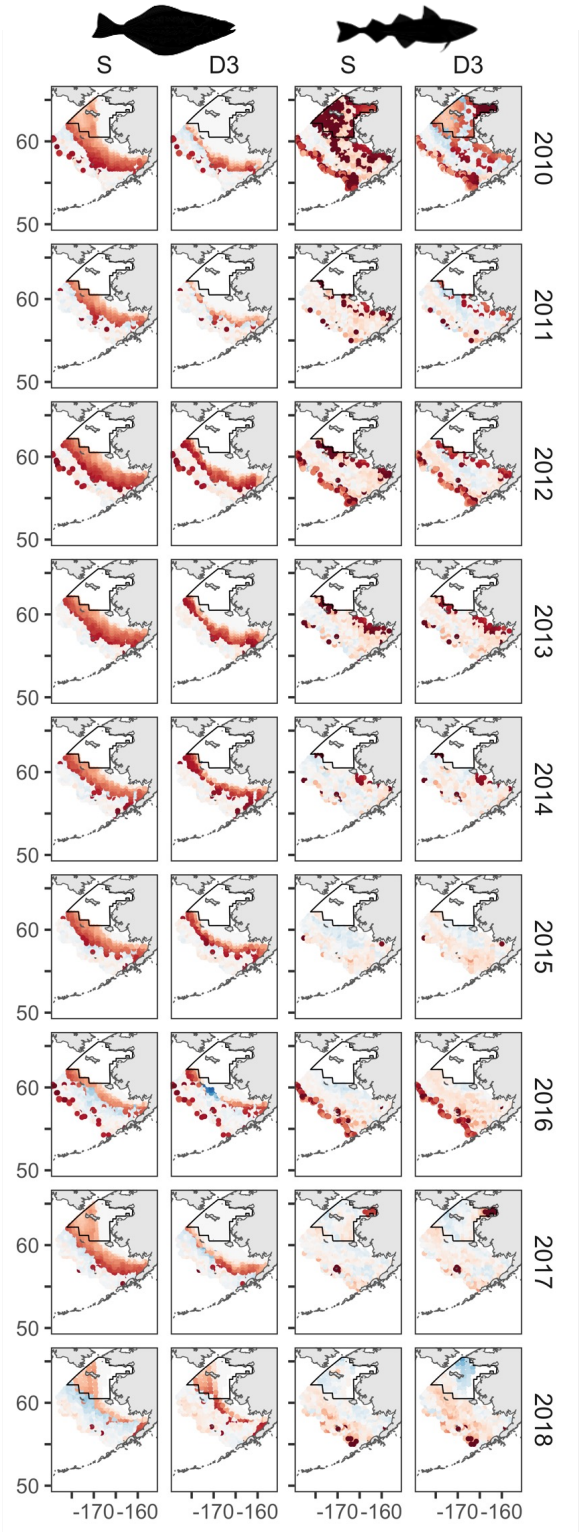

Figure S15 (cont'd). Standardized residuals from static (S) and complex dynamic (D3) models used to quantify biomass (kg) for Arrowtooth Flounder (left) and Walleye Pollock (right) in the Bering Sea. Years represent 1-yr forecasts beyond the time series fit (*e.g.,* 1992 was forecasted from models fit to data between 1982 and 1991). Blue: models underpredicted relative to observations. Red: models overpredicted relative to observations. The black outlined polygon denotes the northern Bering Sea, which was not regularly sampled in time and space.